Title: Ethanol conversion into olefins and aromatics over HZSM-5 zeolite: Influence of reaction conditions and surface reaction studies

Author: Zilacleide S.B. Sousa Cláudia O. Veloso Cristiane A. Henriques Victor Teixeira da Silva

PII: S1381-1169(16)30072-3
DOI: http://dx.doi.org/doi:10.1016/j.molcata.2016.03.005
Reference: MOLCAA 9804

To appear in: *Journal of Molecular Catalysis A: Chemical*

Received date: 12-10-2015
Revised date: 16-2-2016
Accepted date: 1-3-2016

Please cite this article as: Zilacleide S.B.Sousa, Cláudia O.Veloso, Cristiane A.Henriques, Victor Teixeira da Silva, Ethanol conversion into olefins and aromatics over HZSM-5 zeolite: Influence of reaction conditions and surface reaction studies, Journal of Molecular Catalysis A: Chemical http://dx.doi.org/10.1016/j.molcata.2016.03.005

Ethanol conversion into olefins and aromatics over HZSM-5 zeolite: influence of reaction conditions and surface reaction studies

Zilacleide S. B. Sousa[a,1], Cláudia O. Veloso[b], Cristiane A. Henriques[a,b] and Victor Teixeira da Silva[a*]

[a] *Universidade Federal do Rio de Janeiro, NUCAT, Programa de Engenharia Química, COPPE, P.O. Box 68502, 21941-914, Rio de Janeiro, RJ, Brazil.*

[b] *UERJ, Instituto de Química, Programa de Pós-graduação em Engenharia Química, Rua São Francisco Xavier, 524 Maracanã, 20550-900, Rio de Janeiro,RJ, Brazil.*

** Corresponding author: victor.teixeira@peq.coppe.ufrj.br, Phone: +55 21 3938 8344 Fax: +55 21 3938 8300. Email address: victor.teixeira@peq.coppe.ufrj.br*

[1] *Present address: UERJ, Instituto de Química, Rua São Francisco Xavier, 524 Maracanã, 20550-900, Rio de Janeiro,RJ, Brazil*

Authors e-mails: zilasousa@gmail.com (Z. S. B. Sousa); co.veloso@hotmail.com (C. O. Veloso); cah@uerj.br (C. A. Henriques)

Graphical abstract

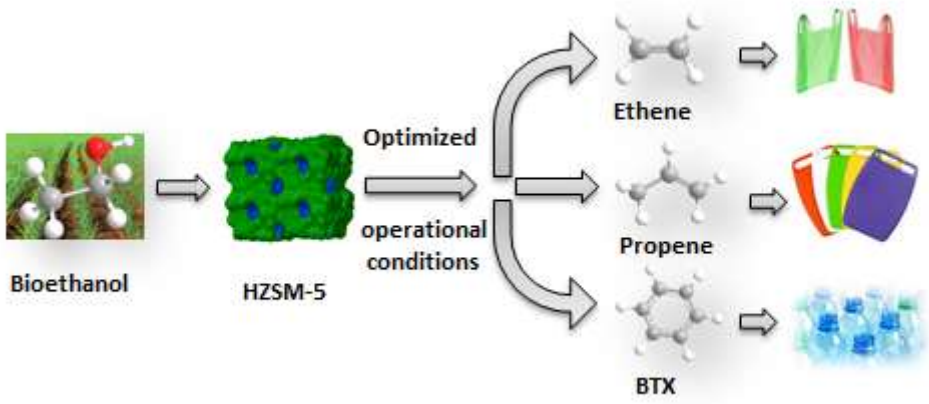

Highlights

- Ethanol can be converted into ethane, propene and aromatics over HZSM-5.
- DRIFTS and TPD data allowed to confirm the reaction route.
- For temperatures lower than 300 ^{o}C the major products are ethane and diethyl ether.
- At T = 500 ^{o}C the ratio propene/aromatics depends on space velocity.

Abstract

Ethanol is an important renewable feedstock that represents an attractive alternative resource for petrochemical industry. In this work, the conversion of ethanol into hydrocarbons, particularly light olefins and aromatics, catalyzed by HZSM-5 was studied under different conditions of temperature (300–500 ºC), partial pressure of ethanol (0.04–0.35 atm), and space velocity (165–0.65 $g_{ethanol}\ g_{cat}^{-1}\ h^{-1}$). At 500 ºC and partial pressure of ethanol equal to 0.12 atm, the formation of propene was favored by an intermediate space velocity (6.5 $g_{ethanol}\ g_{cat}^{-1}\ h^{-1}$), whereas aromatics were favored by the lowest space velocity (0.65 $g_{ethanol}\ g_{cat}^{-1}\ h^{-1}$). The reaction route inferred from the catalytic tests was consistent with that found in the literature and was supported by the surface reaction studies performed by TPD of ethanol and TPSR. In situ DRIFTS of adsorbed ethanol confirmed that the alcohol is adsorbed as ethoxy species on the Brønsted acid sites of the zeolite. With the increase in temperature, the adsorbed ethoxy species form diethyl ether and subsequently ethene confirming that the conversion of ethanol into ethene involves two consecutive steps.

Keywords: Ethanol; Light olefins; Aromatics, HZSM-5, TPD of ethanol; DRIFTS

1. Introduction

The catalytic conversion of ethanol into valuable chemicals such as hydrocarbons, higher chain alcohols, aldehydes, and esters has attracted significant attention from academic and industrial researchers. In the petrochemical industry, ethanol can be used as a green raw material for the production of light olefins (ethene and propene) and aromatics (benzene, toluene and xylenes - BTX) replacing the conventional processes, which are high-energy consuming and based on fossil resources (oil and natural gas). Although the oil price currently shows a downward trend, the political instability in producing countries causes uncertainty in the supply of oil and natural gas. Moreover, environmental protection policies of different countries have encouraged the use of renewable raw materials. Thus, ethanol that can be obtained from the fermentation of molasses (1^{st} generation ethanol) or from lignocellulose biomass, which includes agricultural and forestry residues, by-products of wood transformation industry, and herbal or ligneous plants (2^{nd} generation ethanol), represents an attractive alternative resource for petrochemical industry [1].

In recent years, the transformation of ethanol into hydrocarbons, particularly C_3 - C_4 olefins and BTX aromatics, has attracted considerable attention. Zeolites have been widely studied as catalysts for these reactions. Among them, ZSM-5 zeolites are the most promising catalyst for the transformation of ethanol into petrochemical products [1-6]. These zeolites exhibit acidic and structural characteristics that favor the transformation of ethanol into not only ethene but also C_3 - C_8 hydrocarbons. Moreover, some of their physicochemical properties like acidity, texture, and crystallite size can be tailored by different synthesis routes or pos-synthesis treatments (such as metal incorporation, basic leaching, and steaming) to enhance the selectivity to desired reaction products [1].

The acid properties of ZSM-5 zeolites played an important role in the reaction selectivity to specific hydrocarbon compounds. When ZSM-5 zeolites are compared under similar experimental conditions (reaction temperature, ethanol partial pressure, and contact time), it is observed that a moderate surface acidity favored the production of propene, whereas higher strength and acid sites density favor the formation of aromatic hydrocarbons. On the other hand, ethene is the only product formed over HZSM-5 zeolites with lower acid sites density [5,7-9].

The influence of porous structure on product distribution and catalyst deactivation was discussed by different authors [2, 10, 11]. Madeira et al. [2] and Phung et al. [11] compared HZSM-5 with zeolites having similar Brønsted acid sites density but different porous structure (HFAU, HMOR, HBEA). Despite the differences in the reaction conditions (temperature and pressure), both groups reported that the higher selectivity to C_3^+ hydrocarbons was observed for HZSM-5 whereas the higher production of ethene and diethyl ether was reported for large pore zeolites. Similar trends were reported by Sousa et al. [10] who compared the performance of HZSM-5 and HMCM-22 zeolites with similar SiO_2/Al_2O_3 molar ratios. Although both materials were 10-MR and usually considered as medium pore zeolites, the latter has big cages with 0.71 nm diameter and 1.82 nm height. Again, the zeolite with the more closed pore structure (HZSM-5) presented the higher selectivity to propene and C_3^+ hydrocarbons, ethene being the main product on HMCM-22. The authors mentioned above also observed that the deactivation by coke was slower on HZSM-5 due to the steric restriction imposed by its pore structure on the growth of the coke molecules.

In addition to the physicochemical properties of the zeolites, reaction conditions such as temperature, pressure, and weight hourly space velocity (WHSV) significantly influence catalyst activity and product distribution.

The effect of reaction temperature (300 – 600 ºC) on the conversion of ethanol was investigated by several authors [5,7,9,12,13,14]. Their results indicate that the formation of light olefins (ethene and propene) was favored by the increase in reaction temperature since higher temperatures promoted the dehydration of ethanol to ethene and its oligomerization to higher hydrocarbons, which yielded more ethene and propene by subsequent cracking. On the other hand, the selectivity toward liquid hydrocarbons passed through a maximum at temperatures between 400 ºC and 500 ºC because above this temperature, liquid hydrocarbons decreased as a result of cracking reactions, and methane and coke content increased. However, the optimum temperature to produce each fraction varied among the different authors probably due to differences in the chemical composition of the studied zeolites (silica/alumina ratio - SAR) and experimental conditions (WHSV and ethanol partial pressure).

The influence of contact time (1/WHSV) was strongly dependent on the acid sites density of the zeolite. For short contact times, ethene was the main product

regardless the framework SAR of the zeolite. For an HZSM-5 with lower acid sites density (framework SAR of 280, for example) the yield of ethene decreases continuously with increasing contact time, whereas the yields of propene and butenes increased. The formation of aromatics was not observed over this zeolite [10]. On the other hand, for zeolites with lower SAR, ethene was the only product for short contact times, but an increase in contact time decreased ethene yield, whereas the yield of propene and butenes increased passing through a maximum, and those of C_5^+ aliphatics and aromatics increased [5,8,9,12]. Thus, these results suggested that secondary reactions of oligomerization, hydrogen transfer and cracking were favored by enhanced contact time. These reactions were also favored by the increase in reaction pressure as reported by Costa et al. [9] who observed the raise in paraffin and aromatic contents and the reduction in olefin content with the increase in this parameter. Pressures around 30 bar were used to produce distillate-range hydrocarbons with a petrochemical characteristic through the transformation of ethanol into hydrocarbons over zeolites. On zeolite HZSM-5 (SAR = 40), the main products were paraffins and aromatics from C_5 to C_{11}. High yields of C_3^+ hydrocarbons and low amounts of ethene and diethyl ether were obtained [2,15,16].

Based on the product distribution observed in the catalytic tests, different reaction routes have been proposed in the literature for ethanol conversion over zeolites [1]. The most commonly accepted route involves the intermolecular dehydration of ethanol to ethyl ether, followed by the dehydration of the latter to ethene (at higher temperatures, ethene can also be formed directly by intramolecular dehydration). Then, ethene undergoes successive reactions like oligomerization, cracking, cyclization and aromatization to form higher hydrocarbons [1,2,5,17,18]. Some difference among the routes found in the literature relies on the mechanism of propene formation. Ingram and Lancashire [19] proposed that propene is formed from the cracking of C_6 olefins (produced by ethene oligomerization) whereas Takahashi et al. [8] proposed that carbene species be the transient intermediate in the direct production of propene from ethene.

As part of an extensive research on the conversion of ethanol into hydrocarbons, in this work we investigate ethanol conversion over HZSM-5 zeolite (SAR = 25) under different reaction conditions such as reaction temperature, ethanol partial pressure

(p_{EtOH}), and space velocity (WHSV). The results were discussed regarding ethanol conversion and product distribution. They allowed the selection of the best condition to produce light olefins (mainly propene) or aromatics (BTX). Additionally, temperature programmed desorption (TPD), temperature programmed surface reaction (TPSR) and *in situ* diffuse reflectance infrared Fourier transform spectroscopy (DRIFTS) of ethanol were performed to provide further insights to support the reaction route proposed from the catalytic tests and to confirm the nature of the species adsorbed on HZSM-5 active sites.

2. Experimental

2.1 Catalyst

The HZSM-5 zeolite, supplied by CENPES/PETROBRAS (Rio de Janeiro, Brazil), had both chemical and framework SAR (SiO_2/Al_2O_3 molar ratio) values equal to 25 (nominal value), as well as a micropore volume of 0.165 $cm^3\ g^{-1}$. More information on the physicochemical characteristics of this zeolite can be found in a previous work [10].

2.2 Catalytic Evaluation

Ethanol conversion was studied in a fixed-bed flow micro-reactor under atmospheric pressure. Ethanol vapor was generated by passing an N_2 stream through a saturator maintained at a constant desired temperature by means of a thermostatic bath, and then to the reactor containing the catalyst. The catalytic tests were carried out at 200, 300, 400, and 500 °C with a partial pressure of ethanol of 0.04, 0.12, 0.20 and 0.35 atm and a space velocity of 0.65, 6.5, 65 and 165 $g_{EtOH}\ g_{cat}^{-1}\ h^{-1}$. The reactor effluent was analyzed by an *online* gas chromatograph (with a 30-m HP-Plot/Q capillary column and a flame ionization detector). Before the catalytic evaluation, the zeolite was thermally pre-treated to eliminate water and other adsorbed species, using a flow of N_2 (50 mL min^{-1}) ramped from room temperature up to 500 °C at a heating rate of 2 °C min^{-1} and then kept at this temperature for 1 h.

2.3 Temperature-programmed desorption of ethanol (TPD-ethanol)

A home-made instrument equipped with an online quadrupole mass spectrometer (Balzers QMS 422) was used in this study. The samples were pretreated at 500 °C for 1 h under flowing He (30 mL min^{-1}) and then cooled down to 25 °C. Ethanol was chemisorbed at room temperature by passing He (60 mL min^{-1}) through a saturator containing ethanol for 30 min. Afterward, the sample was purged for 1 h in He flow (60 mL min^{-1}) to remove any physically adsorbed ethanol, and then the temperature was increased at a heating rate of 10°C min^{-1} up to 500 °C. The desorbing species were continuously monitored by their characteristic mass fragments (m/e): 46 (ethanol), 24 (ethene), 59 (diethyl ether), 18 (water), 2 (hydrogen), 43 (acetaldehyde), 40 (olefins C3-C4), 78 (benzene), and 91 (toluene). The intensities were corrected to account for the contributions of different compounds.

2.4 Temperature-programmed surface reaction (TPSR ethanol)

Temperature-programmed surface reaction measurements were carried out using the same apparatus used for the TPD of ethanol. Initially, the sample was pretreated in situ, as described in section 2.3. Then, the sample was cooled down to 50 °C and the ethanol/He mixture (60 mL min^{-1}) was fed to the reactor. The temperature was increased at a heating rate of 5 ºC min^{-1} up to 500 °C. The reaction products were collected at temperatures of 50, 100, 150, 200, 250, 300, 350, 400, 450 and 500 °C. The desorbing species were monitored by their characteristic mass fragments (m/e): 46 (ethanol), 24 (ethene), 59 (ethyl ether), 18 (water), 2 (hydrogen), 43 (acetaldehyde), 40 (olefins C3-C4), 78 (benzene), and 91 (toluene). The results were corrected to eliminate interferences from other compounds.

2.5 In situ Diffuse Reflectance Infrared Fourier Transform Spectroscopy (DRIFTS)

In situ DRIFTS analyses were carried out using a Perkin Elmer Spectrum 100 spectrometer equipped with an MCT-A detector and a high-temperature chamber (Harrick) with ZnSe windows. Spectra were acquired at a resolution of 4 cm^{-1} and 150 scans. The zeolite was pre-treated under He flow (30 mL min^{-1}) from room temperature to 500 °C at a heating rate of 5 °C min^{-1}. Then, the zeolite was cooled down to 40ºC, and a stream of saturated ethanol/He was introduced into the chamber, which was maintained at a temperature of 40 °C for 30 min. After removing the reversibly

adsorbed ethanol using a flow of He (30 mL min^{-1}), the catalyst was heated to different temperatures (100, 150, 200, 250, 300, 400 and 500 °C) under He flow. Spectra were acquired at the end of the ethanol adsorption step and at each of the temperature stages. The spectrum of the treated zeolite was used as background.

3. Results and Discussion

3.1. Effect of temperature

The influence of reaction temperature was evaluated in catalytic tests in which the partial pressure of ethanol (0.12 atm) and space velocity (6.5 $g_{EtOH}\ g_{cat.}^{-1}\ h^{-1}$) were kept constant. At temperatures of 300, 400, and 500 °C, the ethanol conversion was complete, while at 200 °C the conversion was only approximately 40 %. Figures 1 to 4 show the product distribution for each temperature. Table 1 compares the distribution of products formed at a reaction time of 10 min, when the possible effects of deactivation of the catalytic sites by coke formation were insignificant.

Figure 1 and Table 1 show that when the reaction was conducted at 200 °C, ethyl ether (DEE) was the main product, followed by the formation of ethene. At this temperature, no change was observed in the conversion of ethanol, which remained at 40 %, or in the distribution of products (only ethene and ethyl ether), throughout 15 h of reaction. To evaluate the effect of ethanol conversion on the product distribution, an additional catalytic test was performed at 200 °C and 1.3 $g_{EtOH}\ g_{cat}^{-1}\ h^{-1}$. Under these conditions, ethanol conversion reached 60 %. Although the amount of ethene increased, DEE was still the main product formed. These results suggested that at this temperature, the conversion of ethanol into ethene mainly took place via the route including ethyl ether as an intermediary.

At 300 °C, the conversion of ethanol was complete and the formation of DEE was no longer observed (Table 1). Ethene was the main product formed (87 %), along with small amounts (<5 %) of propene, butenes, and C_6^+, which decreased along the reaction and became negligible after 6 h. Thereafter, ethene was the only product (99 %).

At 400 °C and after a short time on stream (TOS = 10 min) the formation of propene, paraffins ($C_2 - C_4$), and the C_5 ($C_5 - C_5^=$) fraction was favored at the expense of ethene (Table 1). Figure 3 shows that the formation of ethene declined slightly during

the first 6 h of the reaction, passed through a minimum and then increased, while the formation of propene, butenes, and paraffins showed the inverse behavior.

The product distribution at the beginning of the reaction at 500 °C indicated that the formation of propene, butenes, aromatics, and paraffins was favored with increasing reaction temperature. The increase of propene yield with increasing temperature up to 500 °C has also been reported by different authors [5,7] for the conversion of ethanol catalyzed by HZSM-5. Concerning the yields of aromatics and paraffins literature claims that they pass through a maximum at intermediate temperatures [5,7,9,12,13,14]. However, in the present work these maxima were not observed probably due the large intervals between the studied temperatures.

Figure 4 reveals that the formation of light olefins, ethene, propene, and butenes decreased smoothly during the first 6 h of the reaction, while the formation of aromatics and paraffins increased slightly. After 6 h, the formation of ethene increased, reaching approximately 70 % of the total amount of product formed at TOS = 15 h. On the other hand, the formation of propene and other hydrocarbons decreased with increasing reaction time.

The results obtained in this work confirm that temperature plays an important role in the product distribution over HZSM-5 zeolites. Assuming the reaction scheme proposed by Inaba et al. [17], at low temperatures (200 °C) the intermolecular dehydration of ethanol occurs, forming ethyl ether, and the subsequent dehydration of ethyl ether produces ethene. An increase in temperature to 300 °C favors the selective formation of ethene, which is apparently formed from the intramolecular dehydration of ethanol, although its formation from DEE cannot be completely ruled out. Considering that ethyl ether was not identified among the reaction products, its formation and subsequent conversion into ethene might occur at very high rates at temperatures above 300 °C. Further increases in temperature favor the oligomerization of ethene to form higher olefins, which then undergo aromatization, hydrogen transfer, and cracking reactions. Thus, the formation of higher hydrocarbons (olefins, paraffins, and aromatics) increases considerably, while the formation of ethene decreases. This effect was enhanced with a further increase in temperature to 500 °C. At this temperature, there is a reduction in the formation of the C_5 and C_6^+ fractions (non-aromatic), probably due to their cracking to lighter fractions.

For reactions carried out at or above 300 °C, although the conversion of ethanol continues to be complete along the reaction, the formation of ethene continuously increases, while the formation of higher hydrocarbons decreases, particularly after 6 h. These results suggest that the strongest acid sites responsible for oligomerization reactions, cracking, aromatization, and hydrogen transfer undergo gradual deactivation during the reaction due to the formation of coke. Weaker acid sites are less susceptible to coking and would remain active to promote the conversion of ethanol into ethene.

3.2. Effect of partial pressure of ethanol

The effect of the partial pressure of ethanol on the product distribution was evaluated in tests conducted at 500 °C and a WHSV of 6.5 $g_{EtOH}\ g_{cat}^{-1}\ h^{-1}$. The influence of reaction time at each partial pressure is shown in Figures 5 to 7, while Table 2 shows the distribution of products at TOS = 10 minutes. Under the studied conditions, ethanol conversion was complete throughout the reaction (15 h) for all partial pressures investigated. Regardless of the partial pressure of ethanol, ethene was the primary product formed, and the formation of ethyl ether was not observed.

At a partial pressure of 0.04 atm (Figure 5), ethene was the main product. With increased TOS, a slight decrease in ethene formation occurred, which was accompanied by the production of olefins with 3, 4, and 5 carbon atoms. These results were consistent with the fact that oligomerization reactions, which are polymolecular, were not favored at a low partial pressure of the reactants.

The rise in ethanol partial pressure to 0.12 atm favored the formation of butenes, aromatics, paraffins and propene at the expense of ethene. As observed in Figure 4, with increased TOS, the formation of light olefins, ethene, propene, and butenes decreased during the first 6 h, while the formation of aromatics and paraffins slightly increased. After 6 h, the formation of ethene increased, reaching approximately 70 % of the total products formed at the end of the reaction (15 h). On the other hand, the formation of propene and other hydrocarbons decreased with increasing reaction time. A further increase in the partial pressure to 0.20 atm promoted the formation of aromatics and paraffins (C_2-C_4), but there was a slight decrease in the formation of propene. The formation of methane and higher hydrocarbons (C_6^+) was negligible.

At a partial pressure of 0.35 atm, a significant reduction in the formation of ethene accompanied by a large increase in the formation of paraffins and aromatics was observed. The formation of propene, butenes, and the C_5 fraction was not influenced by the increase in partial pressure.

As observed in Figures 6 and 7, the effect of TOS on product distribution was similar at partial pressures of 0.20 and 0.35 atm. Thus, with increasing reaction time, the formation of propene and butenes was maximized at approximately 6 h, whereas that of C_2 - C_4 paraffins and aromatics passed through a maximum at shorter reaction times. On the other hand, the formation of ethene continuously increased over time.

The obtained results confirmed that the increase in partial pressure of ethanol favored bi- and polymolecular reactions such as those associated with the formation of higher paraffins and aromatics, as well as reactions related to coke formation. Thus, at shorter reaction times, the formation of propene and aromatics was greatly affected, but at longer TOS, coke formation begins to dominate, deactivating the strong acid sites. The weaker acid sites were less influenced by coke and remained active to promote the conversion of ethanol into ethene.

3.3. Effect of space velocity

The influence of the space velocity on the distribution of products was evaluated in tests conducted at 500 °C and a partial pressure of ethanol equal to 0.12 atm. The influence of TOS on the product distribution is shown in Figures 8 to 10.

Under the studied conditions, ethanol conversion was complete throughout the reaction (15 h). Regardless of the space velocity employed, ethene was the main product, and the formation of ethyl ether was not observed.

Regarding the effect of reaction time on the product distribution, for a space velocity of 165 $g_{EtOH}\ g_{cat}^{-1}\ h^{-1}$ (Figure 10), ethene was the only product formed during the reaction (15 h).

For a space velocity of 65 $g_{EtOH}\ g_{cat}^{-1}\ h^{-1}$ (Figure 9), the product distribution remained stable during the first 5 h of the reaction. Thereafter, the oligomerization of ethene was inhibited, and the formation of propene, butenes, and pentenes decreased simultaneously with the increase in ethene production.

For the space velocity of 6.5 g_{EtOH} g_{cat}^{-1} h^{-1} (Figure 4), as discussed earlier, an increase in TOS led to a decrease in the formation of light olefins, propene and butene. The formation of aromatics and paraffins increased slightly up to TOS = 6 h and then decreased smoothly in an opposite trend to that observed for ethene.

The effect of increased reaction time was significant at a space velocity of 0.65 g_{EtOH} g_{cat}^{-1} h^{-1} (Figure 9). The formation of light olefins (ethene, propene, butenes, and pentenes) increased slightly with time, while the production of aromatics and paraffins slightly decreased. These results reflected the effect of coke formation, which had a significant influence on hydrogen transfer and aromatization reactions.

Figure 11 shows the product distribution as a function of contact time (1/WHSV) under conditions in which the effect of coke deposition was minimized (TOS = 10 min). The formation of ethene continuously decreases with an increase in contact time, whereas the formation of propene and butenes increases, passes through a maximum at 0.2 g_{EtOH} g_{cat}^{-1} h^{-1} and then decreases. The production of C_2-C_4 paraffins and aromatics is favored at higher contact times.

As shown in Figure 11, the gradual decrease in space velocity under conditions in which coke formation can be neglected (TOS = 10 min) initially favored the formation of olefins containing 3 and 4 carbon atoms, and subsequently the production of paraffins and aromatics. Under these conditions (500 °C, 0.12 atm), ethene is the only primary product of the reaction (Figure 11). With increasing contact time, ethene undergoes oligomerization, which leads to the formation of higher olefins that rapidly undergo cracking and form propene and butenes.

For lower space velocities, there is a reduction in the formation of light olefins (which behave as reaction intermediates) and a consequent increase in paraffins and aromatics. This fact confirms that these latter products were generated from olefin oligomerization followed by aromatization, cracking, and hydrogen transfer, in agreement with the scheme proposed by Inaba et al. [17].

Similar trends have been reported by Aguayo et al. [14], who studied the effect of space velocity on the conversion of ethanol to hydrocarbons over an HZSM-5 zeolite with an SAR equal to 48, at 450 ºC. A reduction in space velocity led to an increase in the formation of C_5^+ compounds and paraffins, whereas the production of ethene decreased. The authors also observed that depending on the space velocity, the

formation of propene and butenes could be maximized. At higher space velocities, ethene was the main product.

Taking into account the improvement in the production of light olefins (mainly propene) and aromatics (BTX), the above results indicate that at 500 °C and a partial pressure of ethanol equal to 0.12 atm, two space velocities can be selected: (i) 6.5 g_{EtOH} g_{cat}^{-1} h^{-1}, to maximize the yield of light olefins, particularly propene, and (ii) 0.65 g_{EtOH} g_{cat}^{-1} h^{-1}, to obtain the highest yield of BTX aromatics.

3.4 Surface reaction studies

Aiming at providing further insights to support the reaction route inferred from the catalytic tests (sections 3.1 and 3.3), the compounds desorbed from zeolite surface throughout the ethanol conversion were investigated via temperature-programmed desorption of ethanol (ethanol TPD) and temperature-programmed surface reaction of ethanol (ethanol TPSR). The nature of the species adsorbed on HZSM-5 active sites after ethanol adsorption as well as along the reaction were followed by *in situ* diffuse reflectance spectroscopy (DRIFTS).

3.4.1 Temperature-programmed desorption of ethanol (ethanol TPD)

Temperature-programmed desorption of ethanol was performed to evaluate the primary products associated with the conversion of ethanol catalyzed by HZSM-5 zeolite. Figure 12 shows the TPD profiles after adsorption of ethanol at room temperature. It can be observed that the desorption of molecular ethanol (unreacted ethanol) starts at 70 °C, passes through a maximum at 150 °C, and ends at 250 °C. At 150 °C, the intermolecular dehydration of adsorbed ethanol begins with the simultaneous formation of H_2O and ethyl ether. Until 190 °C, this is the main reaction on the surface of the zeolite.

The simultaneous desorption of ethene and ethyl ether is observed between 190 °C and 250 °C, which confirms the results found in catalytic tests. Thus, at low temperatures (T < 300 °C), the formation of ethene from ethanol would mainly occur via intermolecular dehydration, with ethyl ether as an intermediate. The preferential formation of ethyl ether at lower temperatures was also observed by Decanio et al. [20] using TPD of ethanol adsorbed on Al_2O_3/F. The desorption of propene or higher

hydrocarbons (C_3^+) was not observed, probably due to the absence of ethanol adsorbed at temperatures higher than 300 ºC.

Acetaldehyde and H_2 were not identified among the desorbed species, indicating that ethanol dehydrogenation did not occur on the studied zeolite. The higher density and strength of the acid sites of this zeolite (SAR= 25) should explain these trends, since acetaldehyde and H_2 desorption in TPD of ethanol was reported for catalysts with metallic/oxide sites [21] or HZSM-5 with lower acid sites density (higher SAR) [22].

3.4.2 Temperature-programmed surface reaction (ethanol TPSR)

The conversion of ethanol was also studied by TPSR over the HZSM-5 sample, as shown in Figure 13. It can be observed that between 150 °C and 250 °C, ethanol was transformed into ethyl ether via intermolecular dehydration and ethyl ether successively underwent dehydration to form ethene. Ether formation reached a maximum at 200 °C and subsequently decreased with increasing temperature, whereas ethene gradually increased. Above 300 °C, ethanol was directly converted to ethene and small amounts of higher olefins (propene and butenes).

The conversion of ethanol into hydrocarbons at temperatures below 300 °C begins with the dehydration of ethanol to ethyl ether, which is then dehydrated to ethene, as previously inferred by catalytic tests and confirmed by TPD of ethanol.

$$2\ C_2H_5OH \longrightarrow C_2H_5 - O - C_2H_5 + H_2O$$

$$C_2H_5 - O - C_2H_5 \longrightarrow 2\ C_2H_4 + H_2O$$

At higher temperatures (> 300 ºC), the direct dehydration of ethanol to ethene occurs and ethene is subsequently converted to higher olefins by oligomerization and cracking.

$$C_2H_5OH \longrightarrow H_2O + C_2H_4$$

$$C_2H_4 \longrightarrow (CH_2)_n \longrightarrow C_3H_6 + C_4H_8$$

Differently to what was observed in the catalytic tests, the formation of aromatics was not identified in TPSR experiments at 400 ºC or 500 ºC. The lower ethanol partial pressure (0.08 atm) employed in these experiments could explain these results.

3.4.3 In situ DRIFTS

The infrared spectrum in the region of hydroxyl vibrations (3800 - 3400 cm^{-1}) showed the presence of two bands. The band at 3600 - 3605 cm^{-1} corresponds to OH groups related to Si-(OH)-Al bridging (Brønsted acid sites), and that at 3740 cm^{-1} to the hydroxyl groups of silanol species (Si-OH). After ethanol adsorption at 40 ºC, the band associated with Si(OH)Al disappeared, whereas the band assigned to the silanol groups was only slightly affected, indicating that ethanol preferentially adsorbs on the Brønsted acid sites.

Figure 14 shows the spectra in the region of fundamental vibrations of the reactive intermediates formed on the surface of HZSM-5. The spectra were recorded immediately after ethanol adsorption at 40 °C (spectrum (a)) and after increasing temperature to 100, 150, 200, 250, 300, 400 and 500 °C (spectra (b)-(h), respectively) in flowing helium. Spectrum (a) shows that ethanol adsorption at 40 °C led to the appearance of bands located at 2980, 2935, 2907, 2880, 1450, 1180 and 1060 cm^{-1}. As shown in Table 3, these bands can be ascribed to the different vibrational modes of ethoxy species formed due to the adsorption of ethanol on Brønsted acid sites, which is accompanied by the formation of a water molecule [23-30]. However, the unequivocal rejection of molecular ethanol adsorption was not possible since it presents band at similar positions.

Thus, ethanol can exist on the surface of the zeolite as: (i) ethoxy species formed by the dissociative adsorption of ethanol on the Lewis (cleavage of O - H bond) or Brønsted (cleavage of C - O bond) sites, and (ii) undissociated ethanol molecules.

After the acquisition of the spectrum of adsorbed ethanol at 40 ºC, the temperature was increased under helium flow. At 100 ºC (spectrum (b)), there were no changes in the spectrum in the ranges 3200 – 2800 cm^{-1} and 2800 – 800 cm^{-1}. At 150 ºC, small changes were observed only in the range 2800 – 800 cm^{-1}; the band at 1060 cm^{-1} decreased, and a band at 1142 cm^{-1}, related to C-O stretching in ethyl ether, appeared [31]. Ethyl ether could be formed by the interaction between two adsorbed ethoxy species, as well as by the reaction between an adsorbed ethoxy and an ethanol molecule adsorbed without dissociation [20].

The C-O stretching bands associated with both ethyl ether (1142 cm^{-1}) and ethoxy species (1060 cm^{-1}) disappeared at 200 ºC. Simultaneously, the appearance of the bands at 2988 cm^{-1} and 950 cm^{-1} should indicate the transformation of ethoxy

species into ethene [23]. These results confirm that the conversion of ethanol into ethene involves two consecutive steps, which correspond to ethanol conversion into diethyl ether and subsequently to ethene through the adsorbed ethoxy species.

At 250 ºC, the bands assigned to ethene became less pronounced, and the band at 1450 cm^{-1} disappeared (spectrum (e)). New bands also appeared at 1508 cm^{-1} and 2967 cm^{-1}. According to Tynjälä et al. [24], the band near 2970 cm^{-1} can be associated with ethene conversion into higher hydrocarbons. The band at 1508 cm^{-1}, which decreased with increasing temperature (spectra (e)–(f)), corresponds to polyenic species that would be formed by the dehydrogenation of oligomeric species, as proposed by Lin et al [32]. These authors suggested that the cracking of the adsorbed oligomeric species could lead to the formation of propene and other olefins. With an increase of temperature to 300 ºC, the intensity of the bands related to CH_2 and CH_3 stretching decreased and virtually disappeared at 400 ºC. At 300 ºC, a low-intensity band at 3016 cm^{-1}, assigned to CH stretching of olefinic carbon, was observed. This band disappeared above 400 ºC, similar to the behavior of bands associated with the stretching of methyl and methene groups.

DRIFTS study of adsorbed ethanol strongly suggests that at 40 ºC ethanol was adsorbed on the surface of HZSM-5 as ethoxy species. With increasing temperature, these species reacted, successively forming ethyl ether, ethene and higher hydrocarbons, as observed by TPD and TPSR experiments. In the studied conditions, the unequivocal rejection of dissociative adsorption of ethanol was not possible. Moreover, the formation of chemically adsorbed water was not observed, as also reported by Golay et al. [26], who investigated the reaction of ethanol on γ-Al_2O_3.

5. Conclusions

The transformation of ethanol into hydrocarbons over an HZSM-5 zeolite was investigated under different operating conditions (reaction temperature, partial pressure of ethanol and space velocity). The results show that the studied parameters influenced the yields of propene and aromatics significantly. Considering propene and BTX aromatics as the products of interest, at 500 ºC and partial pressure of ethanol equal to 0.12 atm, two different space velocities must be selected: : (i) space velocity equal to

6.5 g_{EtOH} g_{cat}^{-1} h^{-1} to obtain light olefins, particularly propene; (ii) space velocity equal to 0.65 g_{EtOH} g_{cat}^{-1} h^{-1} to obtain BTX aromatics.

In situ DRIFTS analysis of adsorbed ethanol confirmed that ethanol is adsorbed as ethoxy species on the Brønsted acid sites of the zeolite. Both catalytic tests and surface reaction studies suggest that at lower temperatures, the formation of ethyl ether occurred via intermolecular dehydration, and then it was converted into ethene. On the other hand, at higher temperatures, the direct conversion of ethanol into ethene proceeded by intramolecular dehydration. Subsequently, ethene oligomerization forms heavier olefins, which undergo (i) cracking, producing light olefins (propene, butenes); or (ii) cyclization and hydrogen transfer, forming aromatic and paraffin.

Acknowledgements

The authors acknowledge CNPq and CENPES/PETROBRAS for the financial support. ZSBS thanks CNPq for the DSc scholarship. CAH acknowledges UERJ for the grants (PROCIENCIA Program).

References

[1] A. Galadima, O. Muraza, J. Ind. Eng. Chem. 31 (2015) 1-14.

[2] F. Ferreira Madeira, N.S. Gnep, P. Magnoux, S. Maury, N. Cadran, Appl. Catal. A-Gen. 327 (2009) 39-46.

[3] F. Cherubini, Energy Convers. Management 51 (2010) 1412-1421.

[4] D. Zhang, R. Wang, X. Yang, Catal. Lett. 124 (2008) 384-391.

[5] Z. Song, A. Takahashi, N. Nimura, T. Fujitani, Catal. Lett. 131 (2009) 364-369.

[6] M. Inaba, K. Murata, I. Takahara, K. Inoue, Adv. Mater. Sci. Eng. Sci. (2012) 1-7.

[7] A.K. Talukdar, K.G Bhattacharyya, S. Sivasanker, Appl. Catal. A: Gen 148 (1997) 357-371.

[8] A. Takahashi, W. Xia, Q. Wu, T. Furukawa, I. Nakamura, H. Shimada, T. Fujitani, Appl. Catal. A 467 (2013) 380-385.

[9] E. Costa, A. Uguina, J. Aguado, P.J. Hernández, Industrial Eng. Chem. Process Des. Dev. 24 (1985) 239-244.

[10] Z.S.B. Sousa, D.V. Cesar, C.A. Henriques, V. Teixeira da Silva, Catal. Today 234 (2014) 182-191.

[11] T. K. Phung, L. Projetti Hernandez, A. Lagazzo, G. Busca, Appl. Catal. A: Gen 493 (1015) 77-x.

[12] K.K. Ramasamy, Y. Wang, Catal. Today 237 (2014) 89-99.

[13] K. Murata, M. Inaba, I. Takahara, J. Jpn. Petrol. Inst. 51 (2008) 234-239.

[14] A.T. Aguayo, A.G. Gayubo, A.M. Tarrio, A. Atutxa, J. Bilbao, J. Chem. Technol. Biotechnol. 77 (2002) 211-216.

[15] F. Ferreira Madeira, N. S. Gnep, P. Magnoux, H. Vezin, S. Maury, N. Cadran, Chem, Eng. J. 161 (2010) 403-408.

[16] F. Ferreira Madeira, K. Ben Tayeb, L. Pinard, H. Vezin, S. Maury, Appl. Catal. A: Gen. 443-444 (2012) 171-180.

[17] M. Inaba, K. Murata, M. Saito, I. Takahara, Kinetics Catal. Lett. 88 (2006) 135-142.

[18] K. Inoue, M. Inaba, I. Takahara, K. Murata, Catal . Lett 130 (2010) 14-19.

[19] C.W. Ingram, R.J. Lancashire, Catal. Lett. 31 (1995) 395-403.

[20] E.C. Decanio, J.W. Bruno, V.P. Nero, J.C. Edwards, J. Catal. 140 (1993) 84-102.

[21] S. M. Lima, I. O Cruz, G. Jacobs, B. H. Davis, L. V. Mattos, F. B. Noronha, J. Catal. 257 (2008) 256-268.

[22] R. Barthos, A. Szechenyi, F. Solymosi, J. Phys. Chem. B, 110, (2006) 21816-21825.

[23] P-Y. Sheng, G.A. Bowmaker, H. Idriss, Appl. Catal. A: Gen. 261 (2004) 171-181.

[24] P. Tynjala, T. T. Pakkanen, S. Mustamaki, J. Phys. Chem. B, 102 (1998) 5280-

[25] J. Wan, F. Chang, Y. Wei, Q. Xia, Z. Liu, Z., , Catal. Lett. 127 (2008) 348-353.

[26] S. Golay, R. Doepper, A. Renken, Appl. Catal. A: Gen. 172 (1998) 97-106.

[27] H. Knozinger, B. Stubner, J. Phys. Chem. 82 (1978) 1526-1532.

[28] M.A. Natal-Santiago, J.A. Dumesic, J. Catal. 175 (1998) 252–268.

[29] J.N. Kondo, K. Ito, E. Yoda, F. Wakabayashi, K. Domen, J. Phys. Chem. B 109 (2005) 10969-10972.

[30] K. Rintramee, K. Föttinger, G. Rupprechter, J. Wittayakun, Appl. Catal. B-Environ., 115-116 (2012) 225-235.

[31] G.A.M. Hussein, N. Sheppard, M.I. Zaki, R.B. Fahin, J. Chem. Soc. Faraday Trans. 87 (1991) 2661-2668.

[32] B. Lin, Q. Zhang, Y. Wang, Ind. Eng. Chem. Res. 48 (2009) 10788–10795

Figure 1

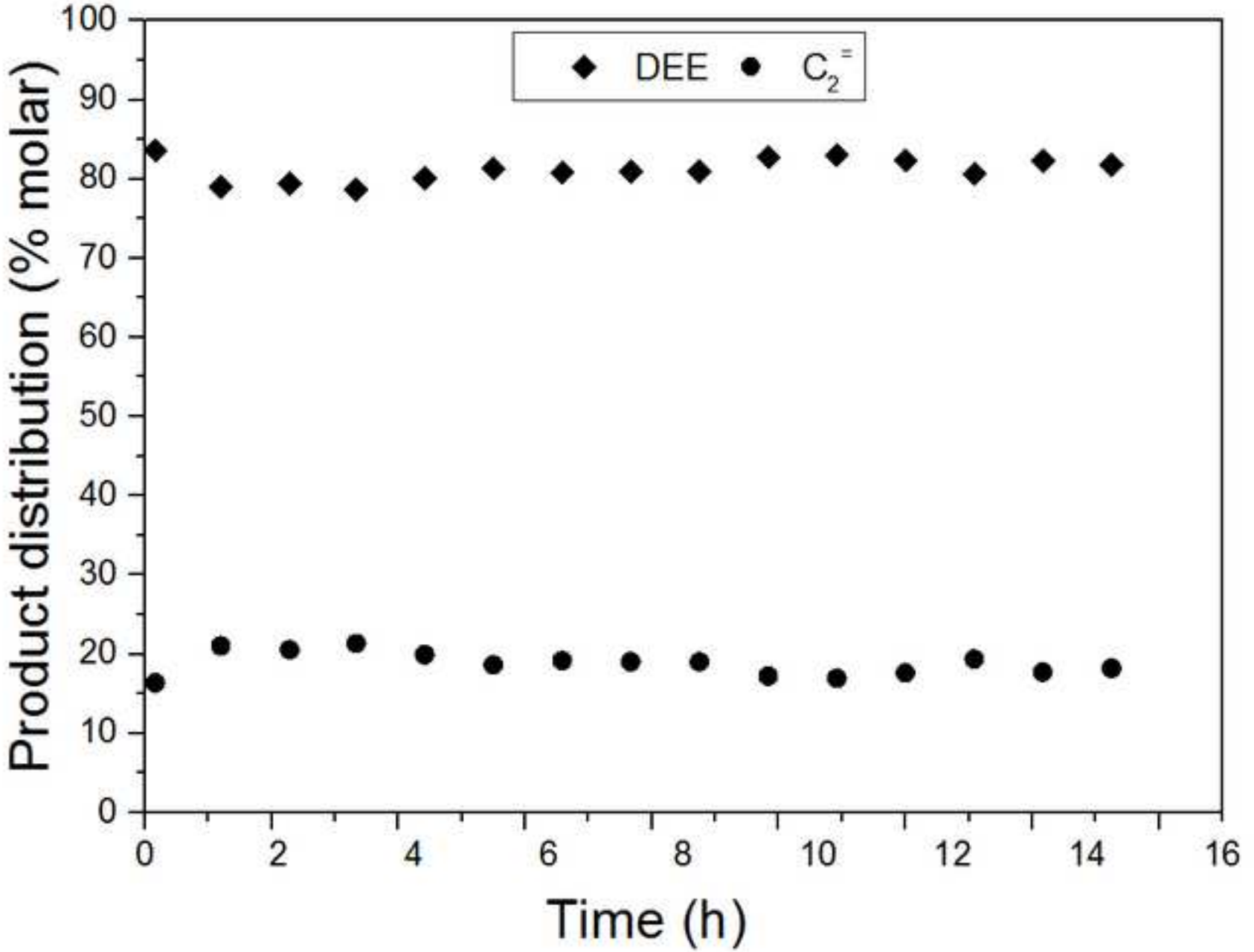
DEE
$C_2^=$
Product distribution (% molar)
Time (h)
0
10
20
30
40
50
60
70
80
90
100
0
2
4
6
8
10
12
14
16

Figure 2

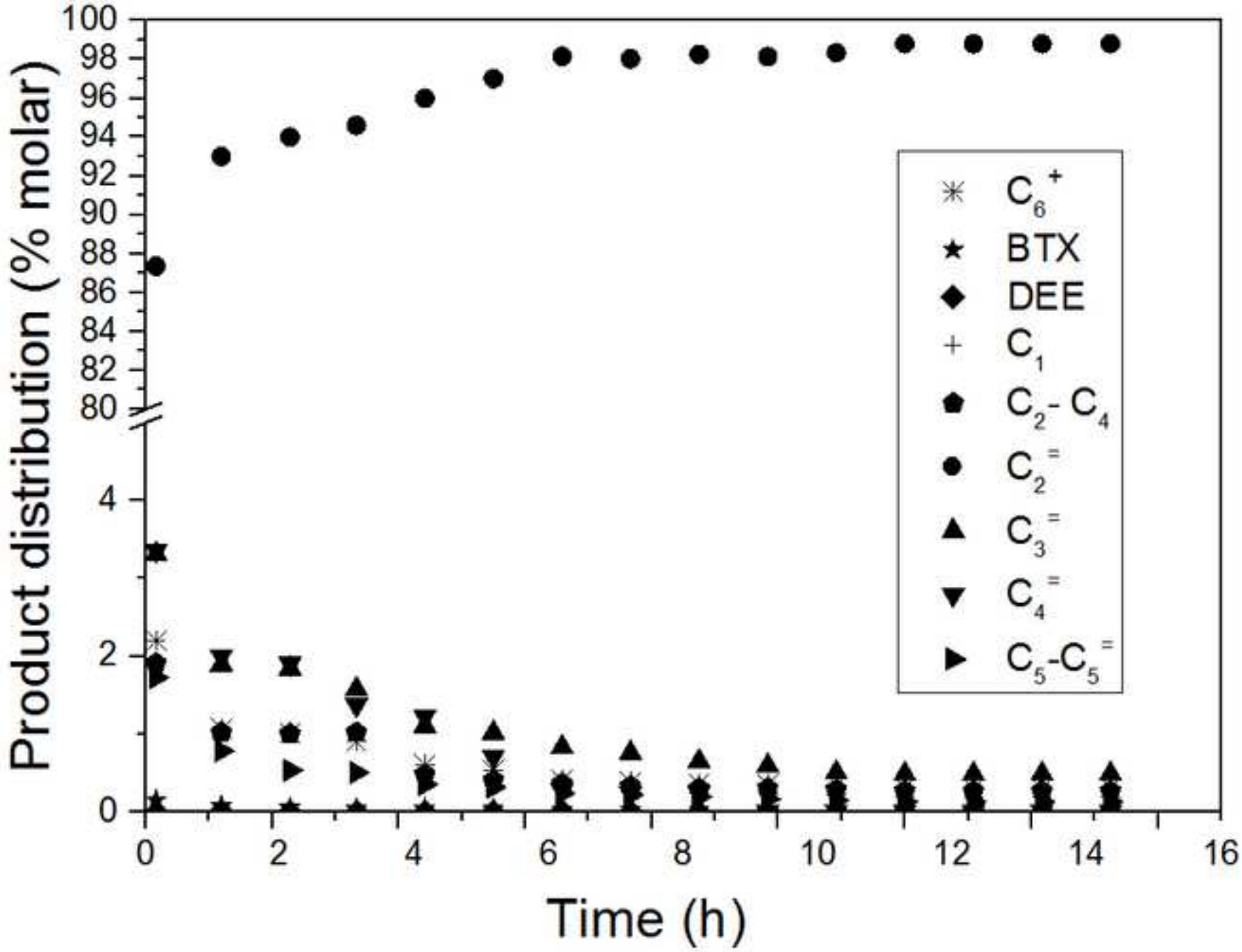
Product distribution (% molar)
Time (h)
100
98
96
94
92
90
88
86
84
82
80
4
2
0
0
2
4
6
8
10
12
14
16
C6+
BTX
DEE
C1
C2- C4
C2=
C3=
C4=
C5-C5=

Figure 3

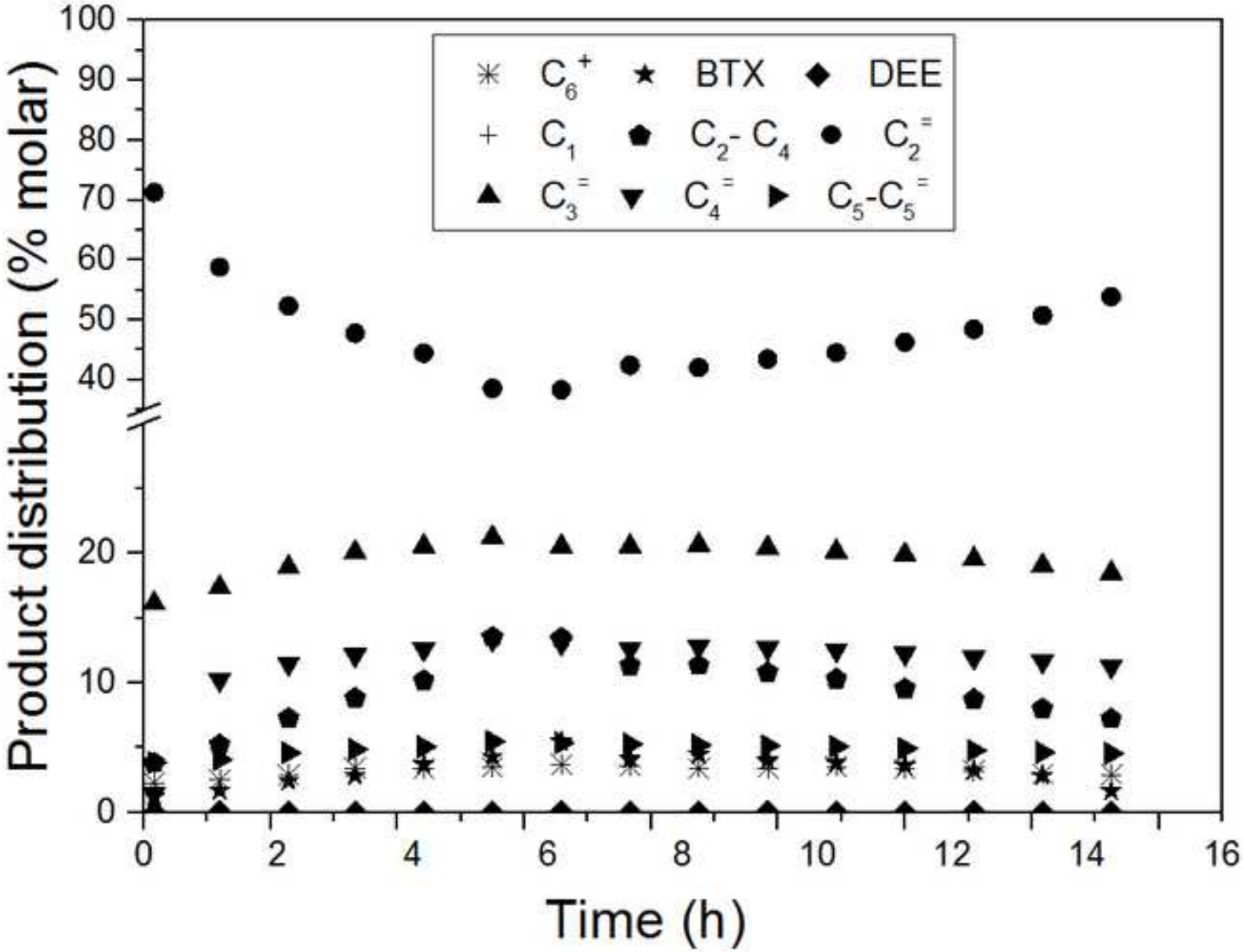
Product distribution (% molar)
Time (h)
C6+
BTX
DEE
C1
C2- C4
C2=
C3=
C4=
C5-C5=
100
90
80
70
60
50
40
20
10
0
0
2
4
6
8
10
12
14
16

Figure 4

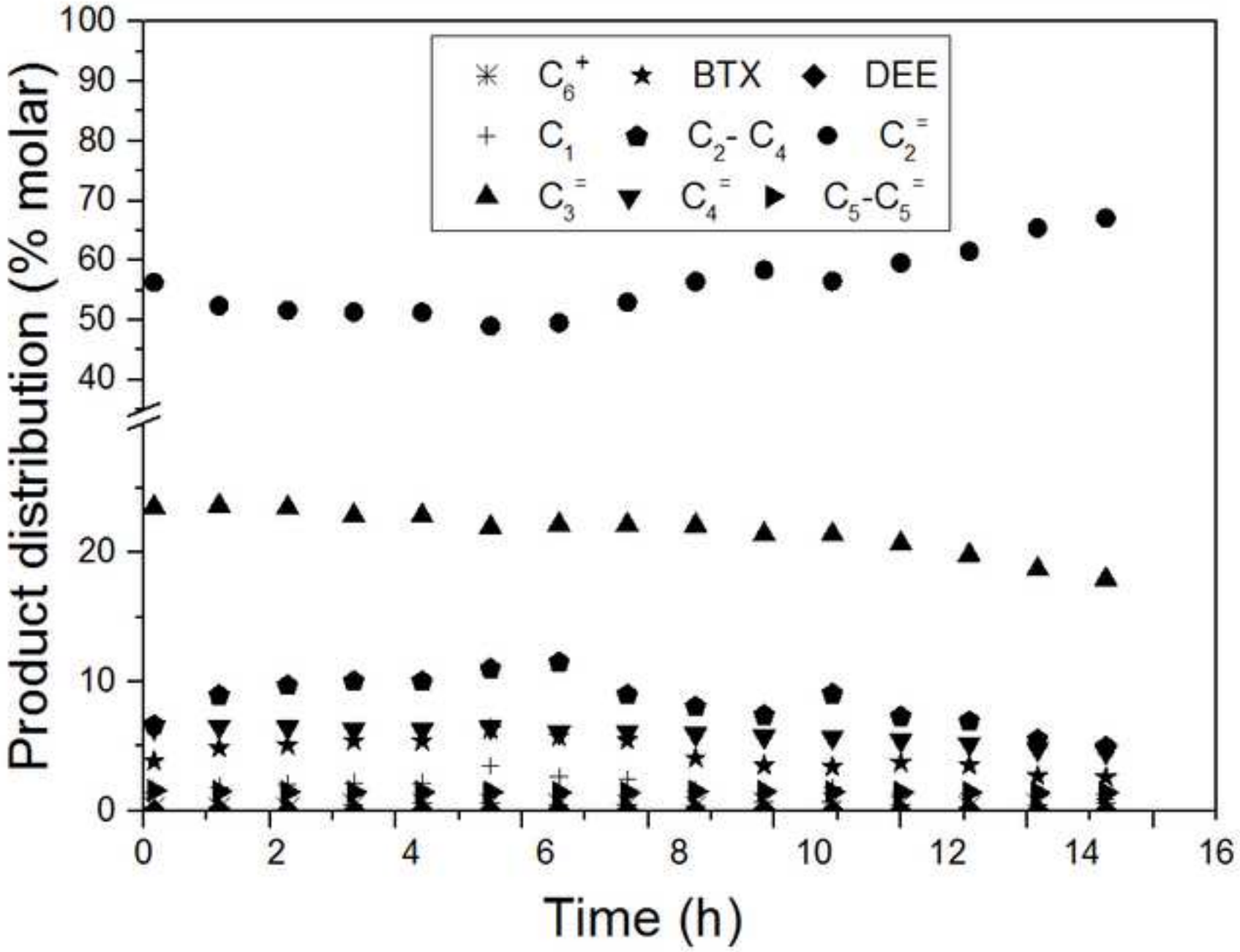
Product distribution (% molar)
Time (h)
C6+
BTX
DEE
C1
C2- C4
C2=
C3=
C4=
C5-C5=
100
90
80
70
60
50
40
20
10
0
0
2
4
6
8
10
12
14
16

Figure 5

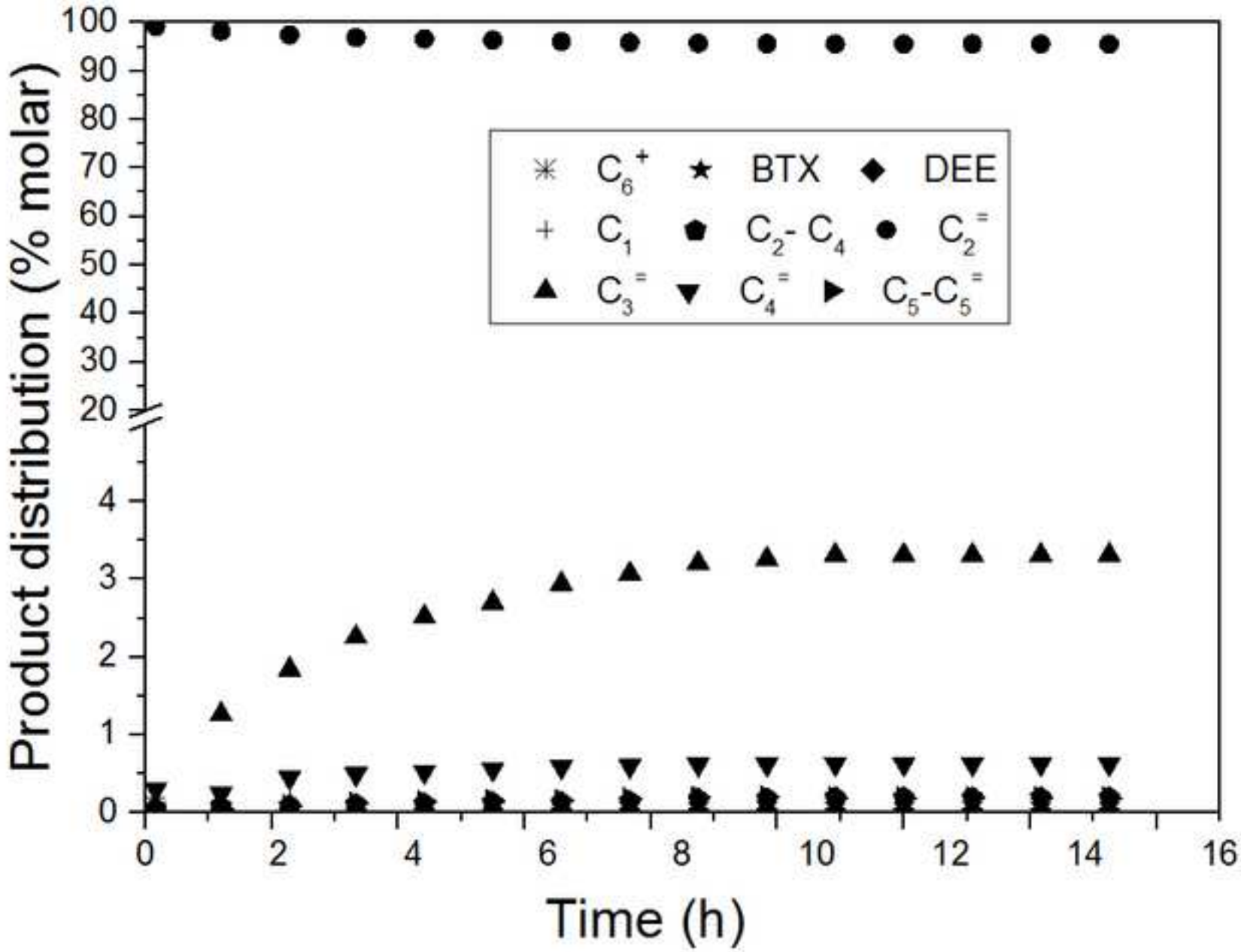
Product distribution (% molar)
Time (h)
C6+
BTX
DEE
C1
C2- C4
C2=
C3=
C4=
C5-C5=
100
90
80
70
60
50
40
30
20
4
3
2
1
0
0
2
4
6
8
10
12
14
16

Figure 6

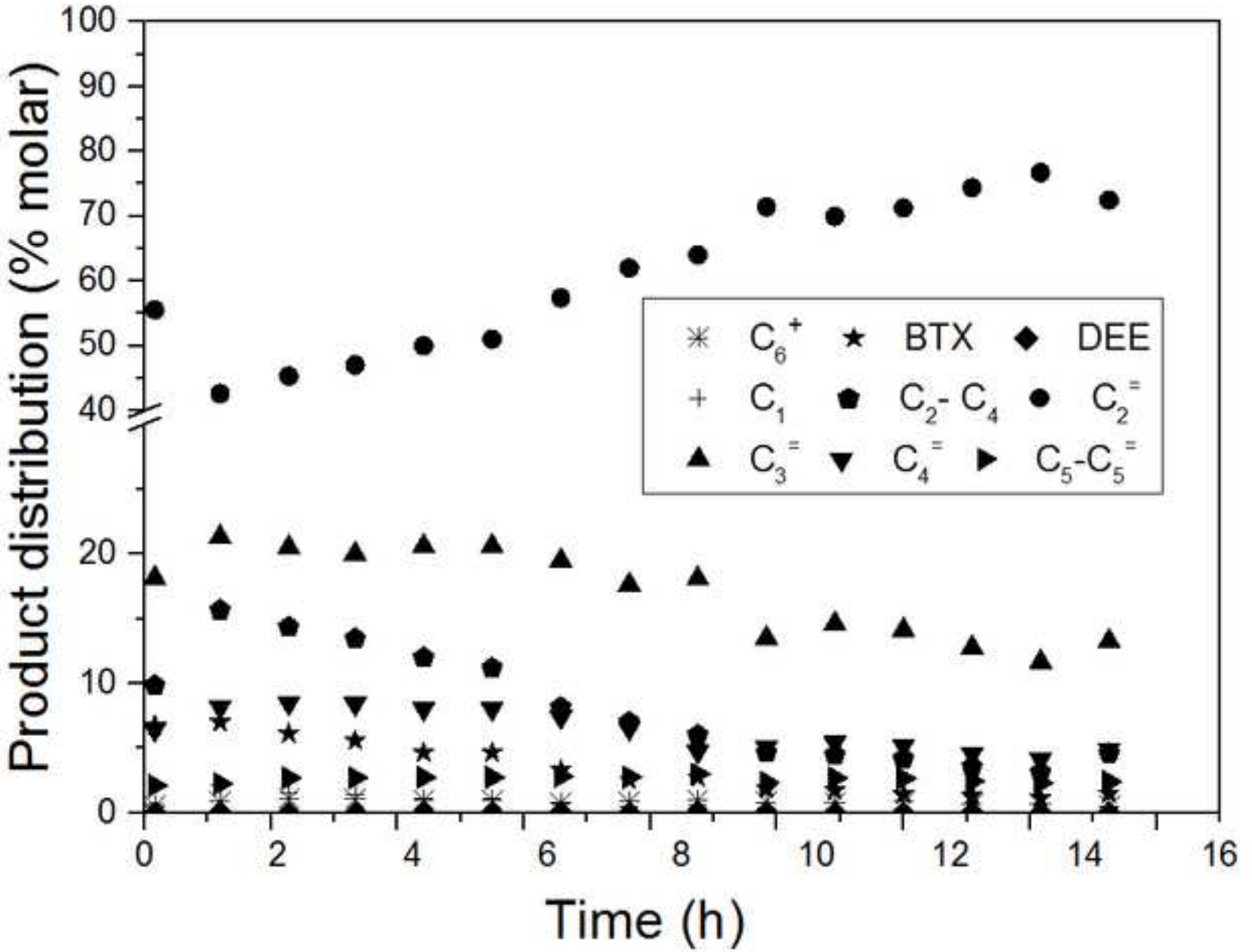
Product distribution (% molar)
Time (h)
0
10
20
40
50
60
70
80
90
100
0
2
4
6
8
10
12
14
16
C6+
BTX
DEE
C1
C2- C4
C2=
C3=
C4=
C5-C5=

Figure 7

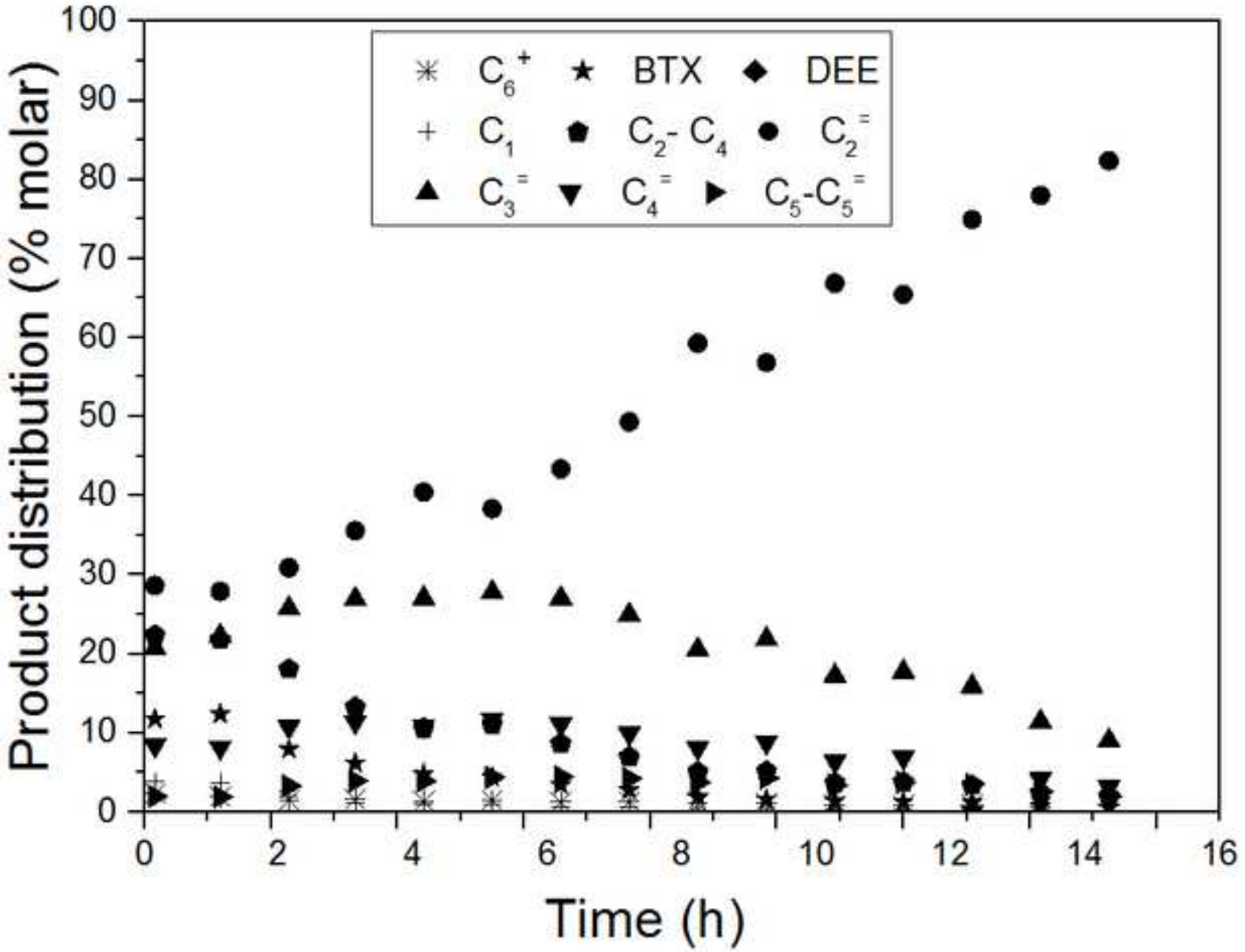
Product distribution (% molar)
Time (h)
C6+
BTX
DEE
C1
C2- C4
C2=
C3=
C4=
C5-C5=
0
10
20
30
40
50
60
70
80
90
100
0
2
4
6
8
10
12
14
16

Figure 8

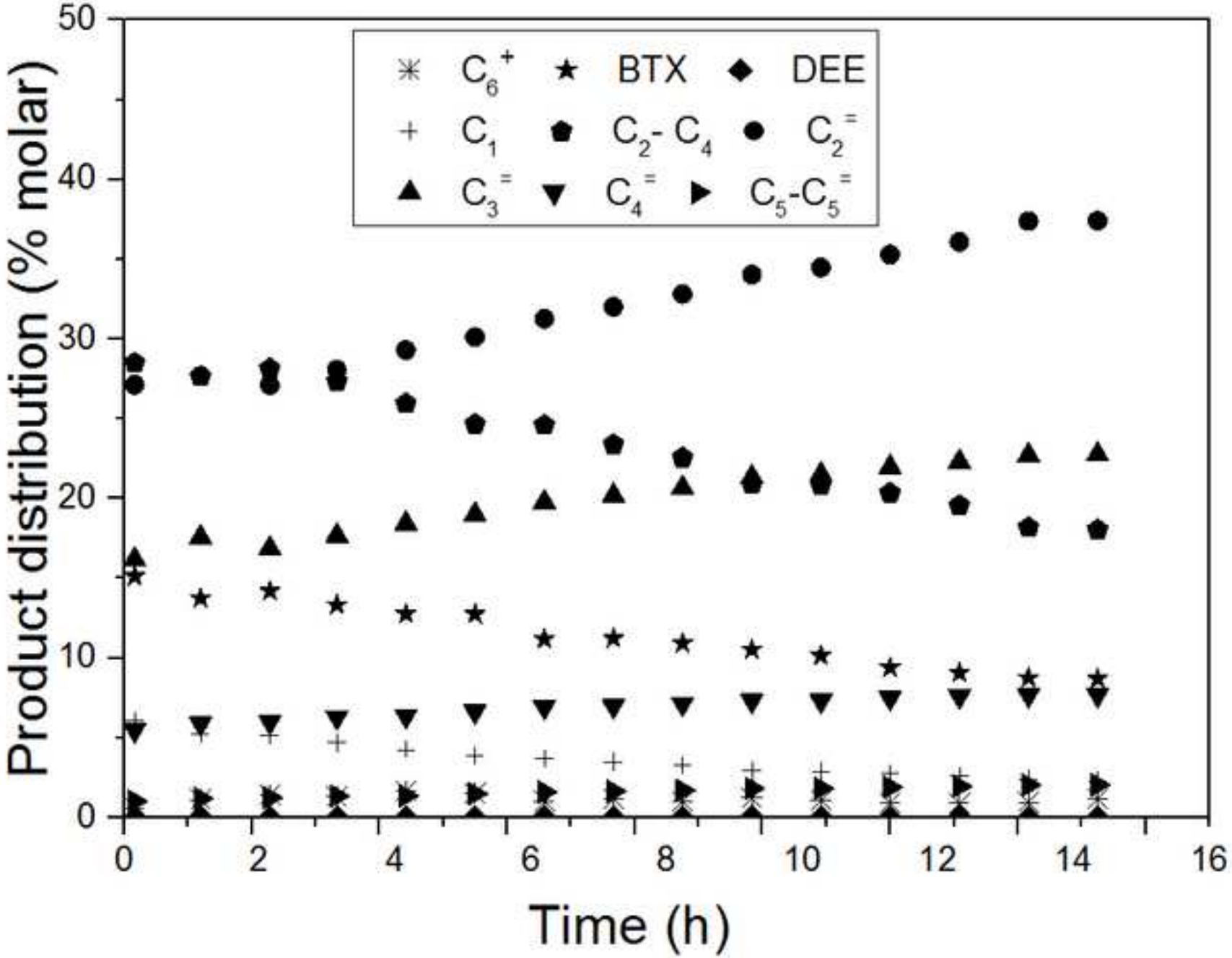
Product distribution (% molar)
Time (h)
0
10
20
30
40
50
0
2
4
6
8
10
12
14
16
C6+
BTX
DEE
C1
C2- C4
C2=
C3=
C4=
C5-C5=

Figure 9

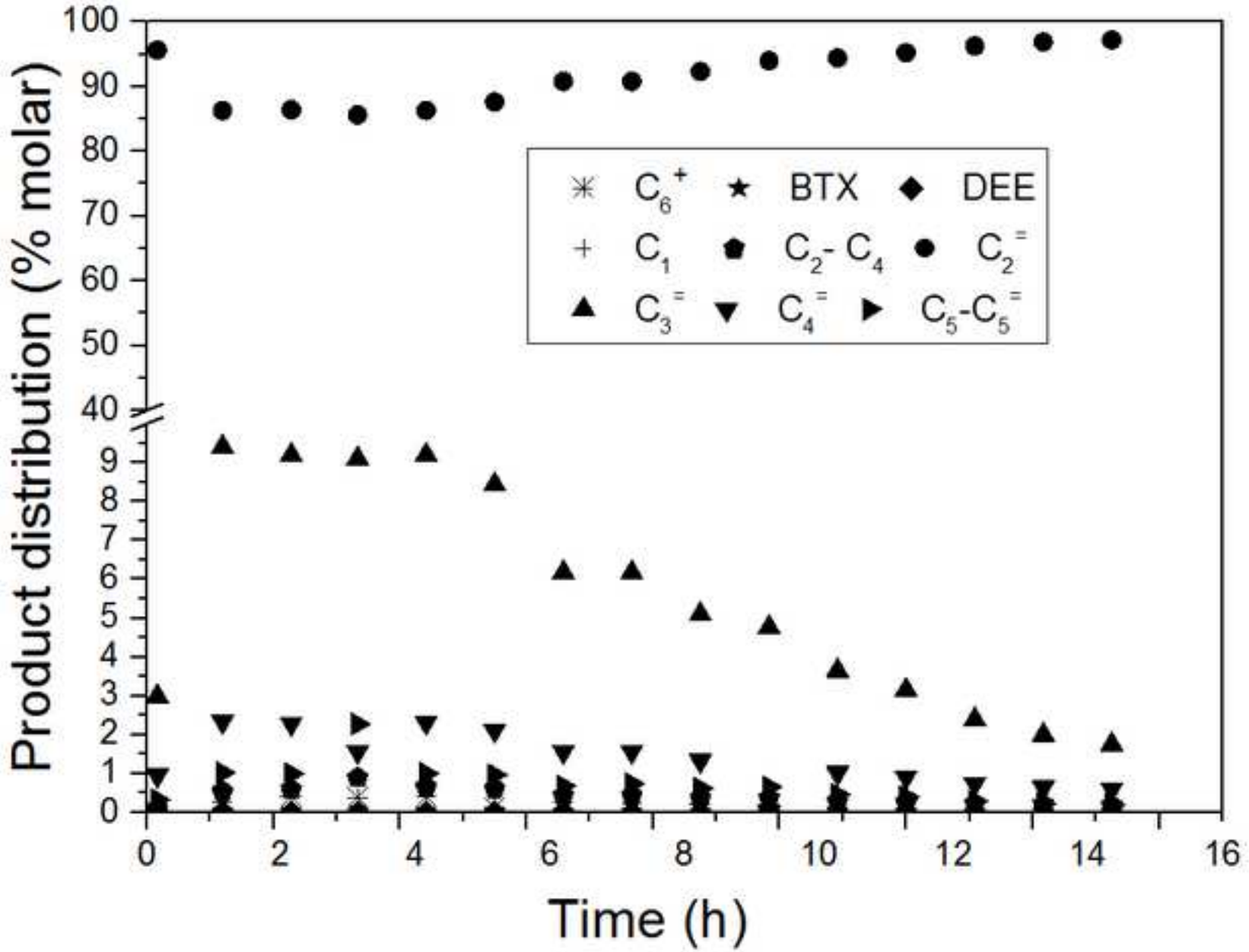
Product distribution (% molar)
Time (h)
C6+
BTX
DEE
C1
C2- C4
C2=
C3=
C4=
C5-C5=
100
90
80
70
60
50
40
9
8
7
6
5
4
3
2
1
0
0
2
4
6
8
10
12
14
16

Figure 10

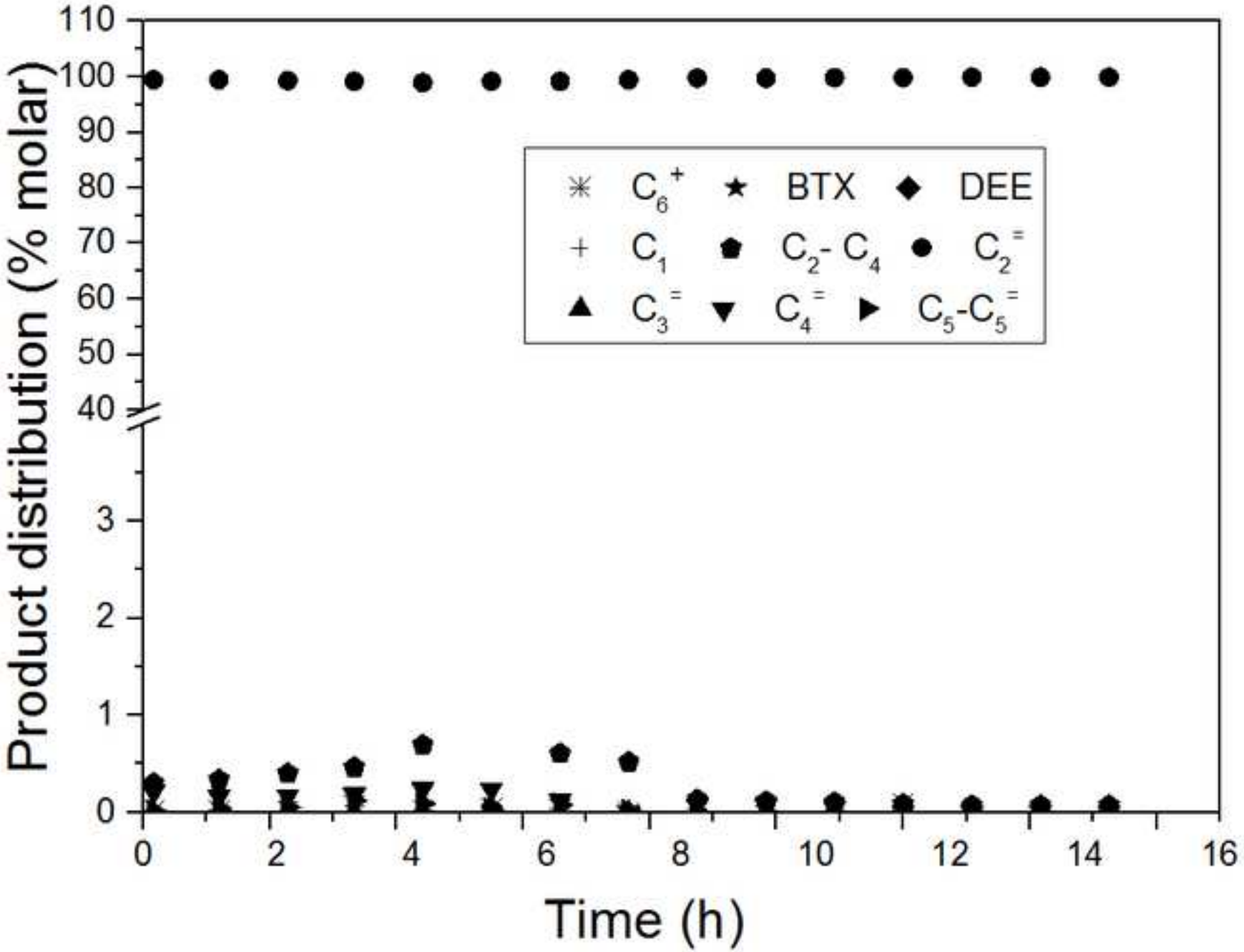
Product distribution (% molar)
Time (h)
110
100
90
80
70
60
50
40
3
2
1
0
0
2
4
6
8
10
12
14
16
C6+
BTX
DEE
C1
C2- C4
C2=
C3=
C4=
C5-C5=

Figure 11

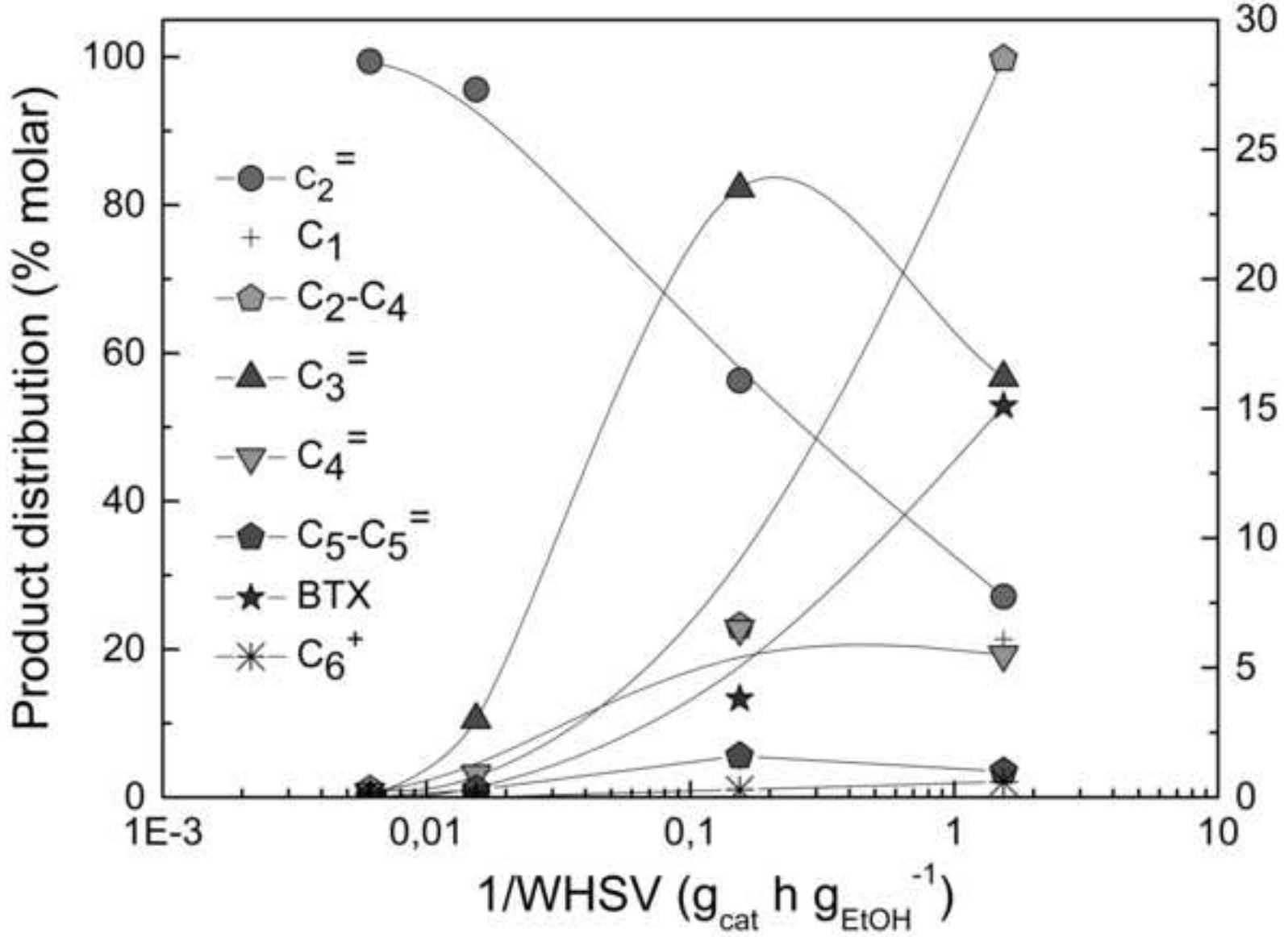
Product distribution (% molar)
100
80
60
40
20
0
30
25
20
15
10
5
0
1E-3
0,01
0,1
1
10
1/WHSV (g_{cat} h g_{EtOH}^{-1})
$C_2^=$
C_1
C_2-C_4
$C_3^=$
$C_4^=$
C_5-$C_5^=$
BTX
C_6^+

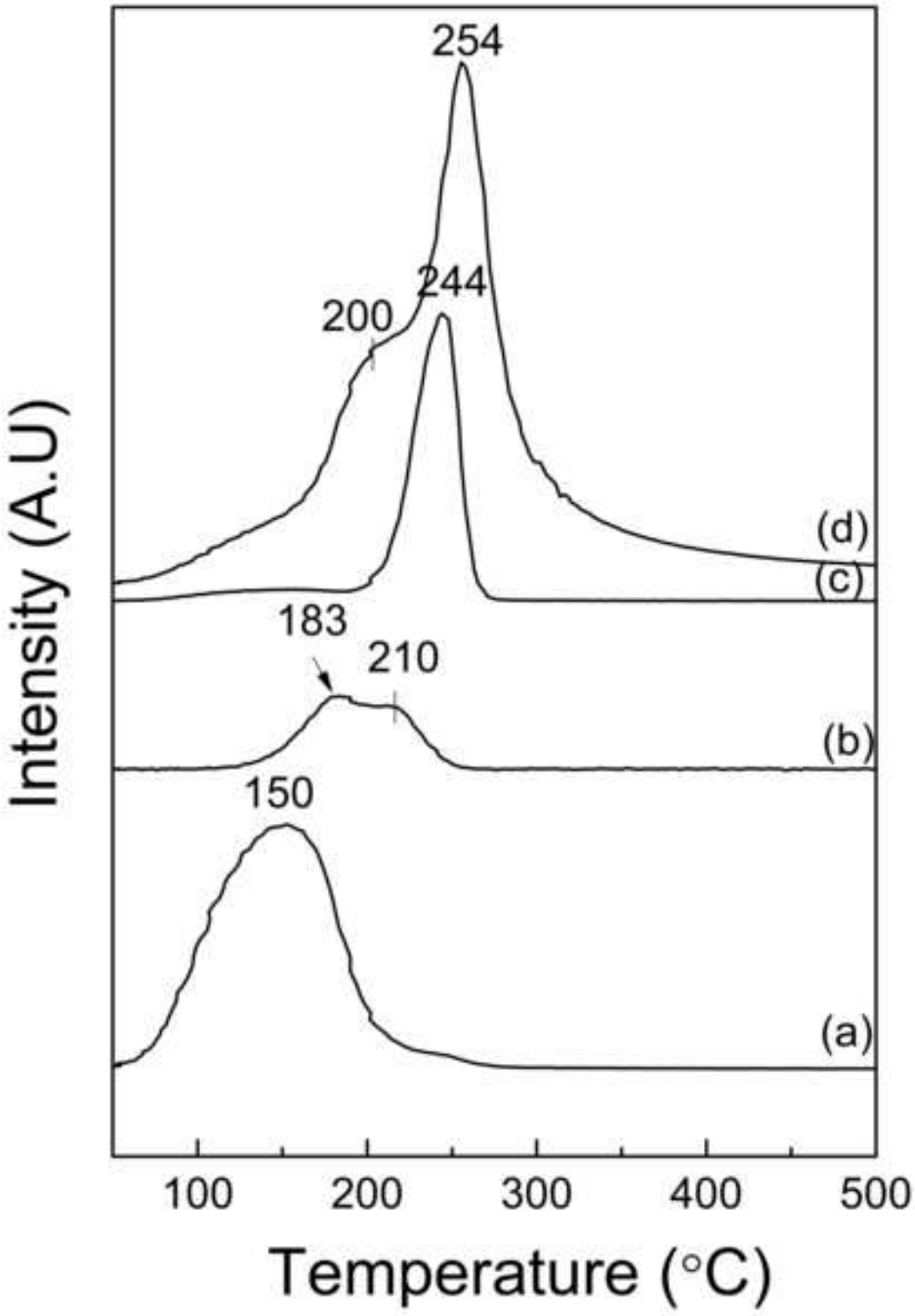

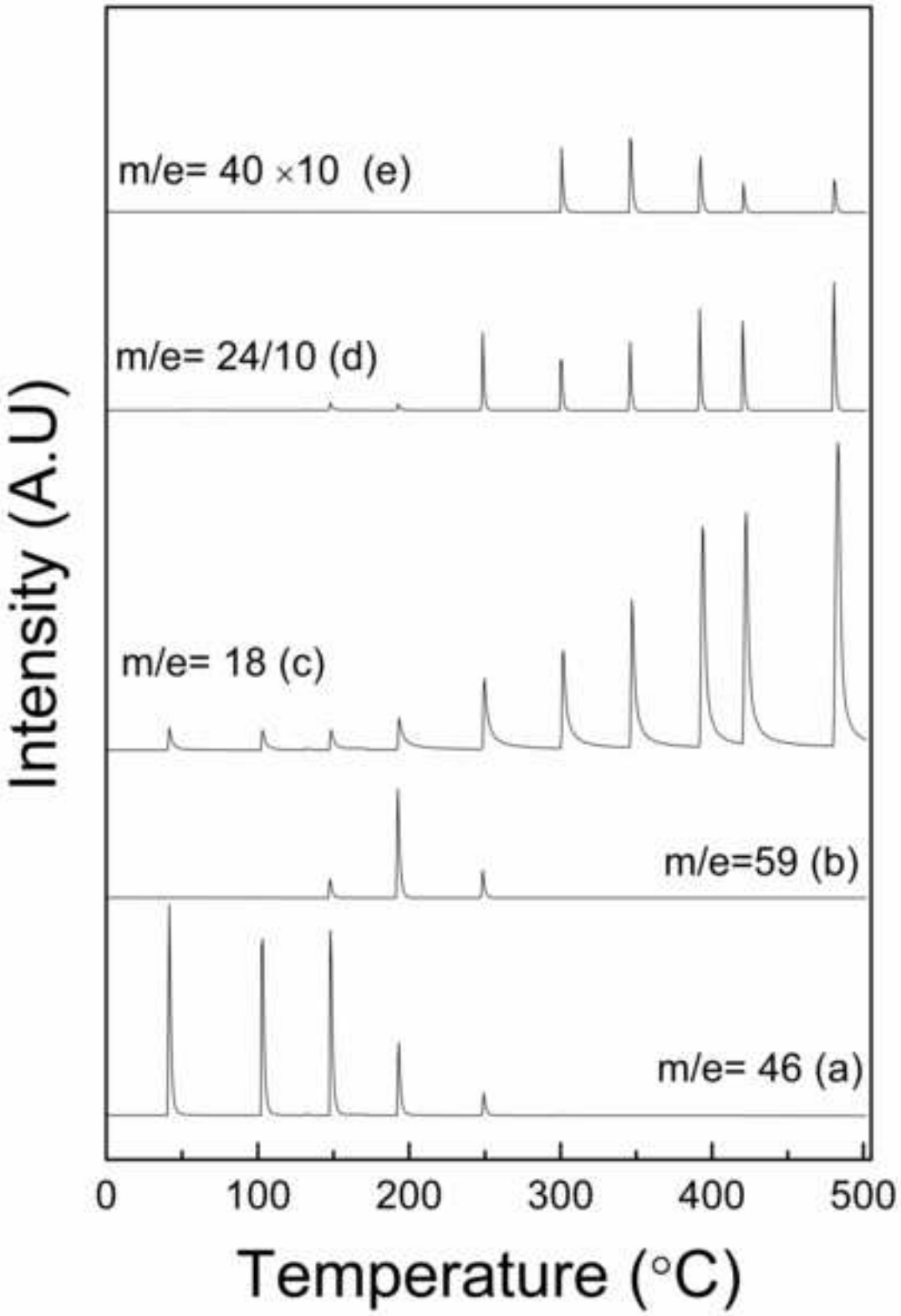

Figure 14

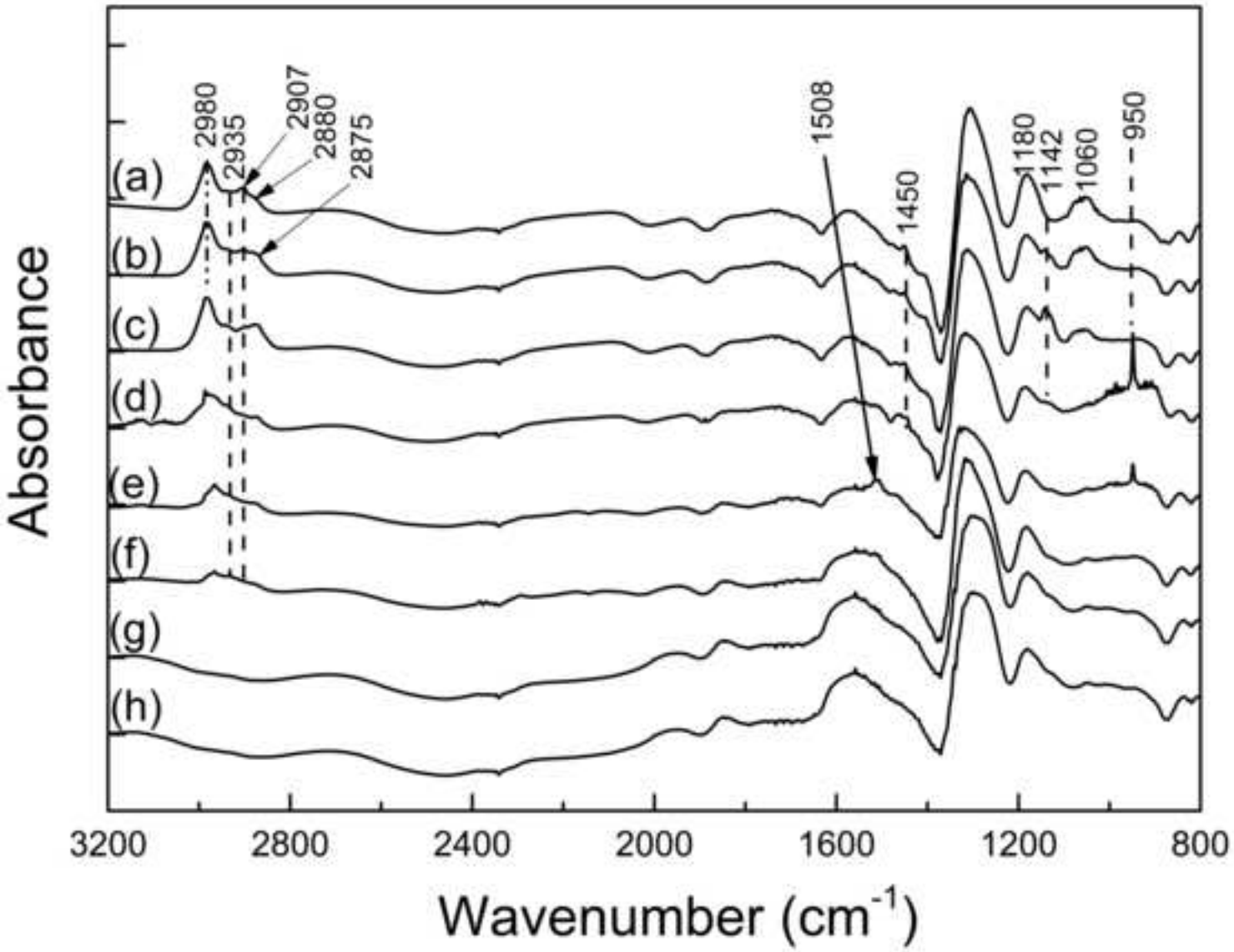
Absorbance
(a)
(b)
(c)
(d)
(e)
(f)
(g)
(h)
2980
2935
2907
2880
2875
1508
1450
1180
1142
1060
950
3200
2800
2400
2000
1600
1200
800
Wavenumber (cm-1)

Table 1. Distribution of the reaction products (% molar) as a function of temperature (TOS = 10 min, p_{EtOH} = 0.12 atm e WHSV = 6.5 $g_{EtOH}\, g_{cat.}^{-1} h^{-1}$).

	200 °C	**300 °C**	**400 °C**	**500 °C**
C_1	0.0	0.0	0.1	1.4
C_2-C_4	0.0	1.9	3.8	6.6
C_2H_6	16.4	87.4	71.2	56.3
C_3H_6	0.0	3.3	16.1	23.5
C_4H_8	0.0	3.4	1.5	6.5
C_5-$C_5^=$	0.0	1.7	3.8	1.6
BTX	0.0	0.1	1.2	3.8
DEE	83.6	0.0	0.0	0.0
C_6^+	0	2.2	2.3	0.3

Table 2. Distribution of the reaction products (% molar) as a function of ethanol partial pressure (TOS = 10 min, T = 500 °C and WHSV = 6.5 $g_{EtOH}\, g_{cat.}^{-1} h^{-1}$).

	0.04 atm	**0.12 atm**	**0.20 atm**	**0.35 atm**
C_1	0.2	1.4	0.6	3.8
C_2-C_4	0.1	6.6	9.9	22.4
C_2H_6	99.2	56.3	55.5	28.6
C_3H_6	0.0	23.5	18.2	20.7
C_4H_8	0.3	6.5	6.4	8.4
C_5-$C_5^=$	0.0	1.6	2,1	2.0
BTX	0.2	3.8	6.8	11.7
DEE	0.0	0.0	0.0	0.0
C_6^+	0.0	0.3	0.5	2.3

Table 3. Attribution of the vibrational bands observed on the DRIFTS spectra of adsorbed ethanol

Band (cm^{-1})	**Attribution**	**Reference**
2988	$=CH_2$ stretching	24
2980	CH_3 asymmetric stretching	23, 25-30
2935	CH_2 asymmetric stretching	23, 25-30
2907	CH_3 symmetrim stretching	23, 25-30
2880	CH_2 symmetric stretching	23, 25-30
1450	CH_3 asymmetrical bending	23, 26,30
1180	C-O stretching	23, 26
1060	C-O stretching	23,26
950	$=CH_2$ bending	24